1 Introduction

Ferromagnets are materials that show long-range magnetic order at the atomic level resulting in parallel alignment of unpaired electron spins within small magnetic regions called *magnetic domains*. The magnetic moment within a domain is the *spontaneous magnetisation* of the material and even exists in the absence of any externally applied field (only below a certain critical temperature called the *Curie temperature* T_{C}, which is an intrinsic property of the material), making ferromagnetic materials unique in their existence. Although spontaneous magnetisation exists in these materials, there is no net magnetic moment for a bulk sample due to random orientation of these tiny magnetic domains with respect to each other. However, once exposed to external magnetic fields, they exhibit high magnetisation due to alignment of the magnetisation in different magnetic domains along the applied field direction. Depending on whether the ferromagnets retain their high magnetisation after removal and reversal of the applied field direction, they may be classified as hard or soft ferromagnets. The soft ferromagnets are ferromagnetic materials that reverse their magnetisation direction almost as soon as the direction of applied field is reversed exhibiting very *low coercivities* (reverse field at which magnetisation is zero) and no *magneto-crystalline anisotropy* as opposed to hard magnets which display very high coercivities. *Permanent magnets* / *hard magnets* are ferromagnetic material that retain their magnetisation once exposed to strong external fields up to large reverse fields and thereby exhibit large *hysteresis* in their magnetic properties. These are normally characterised with a high value of the magnetic energy product, $(BH)_{\mathrm{max}}$, which is a measure of the magnetic energy they can retain. Hence, a permanent magnet can be taken in close analogy to the mechanical spring, which stores mechanical energy whereas a permanent magnet stores magnetic energy [Kir96]. The rare-earth (R) compounds are a special class of permanent-magnet systems, which often achieve high $(BH)_{\mathrm{max}}$.

The name 'rare earth' is a misnomer and originated from scarcity of the element (rare) and the difficulty of extracting these elements from their ores (earth), neither of which is true any more. Discovered in the 1960-70 decade (Fig. 1.1), the rare-earth compounds have proven themselves to be potentially much stronger for permanent-magnet applications than the then-famous Ferrite magnets or the AlNiCos. The maximum energy products achievable with some of the present day rare earth compounds (300–400 $\mathrm{kJ/m^3}$) are many orders of magnitude higher than those for the AlNiCo magnets. The magnetism of the rare earths has been known for several years [Tro90] and particularly their high anisotropy fields [Rad87]. However, the low Curie temperature for all of these elements (well below room temperature – where Gd is an exception with Curie temperature $\simeq$ 20 °C) makes them less attractive for isolated usage as permanent magnets. Alloying these elements with the high-magnetisation, high Curie temperature transition metals (T) results in very attractive permanent-magnet applicants. Some among the popular R-T systems are the Sm-Co compounds, Nd-Fe-B magnets and the Sm-Fe-N system, which have been exploited both in bulk as well as for thin film applications.

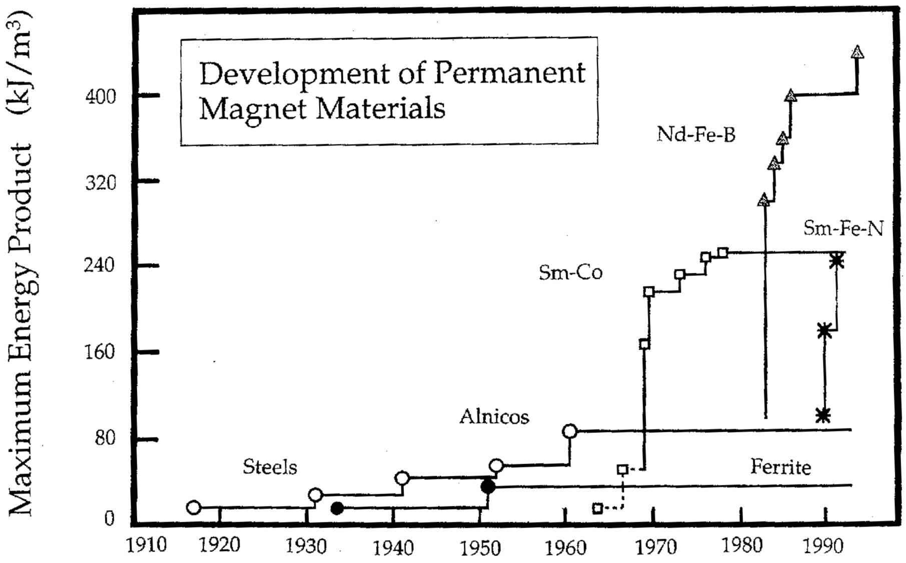

Fig. 1.1: *The improvement in the magnetic energy product over the last century [Coe96].*

A permanent magnet promising high $(BH)_{\mathrm{max}}$ requires high remanence, high coercivity and a well known magnetisation reversal process, all of which must be stable up to high operating temperatures. The upper bound on these properties is superimposed by a crucial interplay between the intrinsic properties of the materials (namely the saturation moment, which decides the maximum remanence that can be obtained, the anisotropy field, which limits the coercivity in the material, and the Curie temperature, which decides the maximum operating temperature of the magnet) and the processed microstructure. Hence, the evolution of novel materials needs a thorough insight into the intrinsic properties of the magnetic material and the processing techniques responsible for a suitable microstructure.

The best exploitation of saturation magnetisation (single domain magnetisation value) in a uniaxial magnet can be done if the material is extremely well textured, such that the whole sample even though still a multi-grain, multi-domain ensemble, behaves essentially as a single grain entity. More appropriately or practically, the realisation of a “single grain” system would be equivalent to a highly textured material, where the grain misalignment is tolerably tiny. In this case, epitaxial films are one very plausible solution. Additionally, an epitaxial growth that forces the easy magnetisation axis to be aligned along only one substrate axis, would bring the system exhibiting uni-axial anisotropy closest to its natural state and suitable for any further investigations. This film as a highly textured magnet has a remanent moment equal to the saturation moment along the easy axis as depicted in Fig. 1.2 and the hard axis contains no remanence or ideally no hysteresis. The realisation of nicely textured films where all the magneto-crystalline energy is stored only along one easy axis was one important task of this work.

The permanent magnet material under investigation is the Sm-Co system. Figure 1.1 confirms the capability of Sm-Co compounds in providing extremely high $(BH)_{\text{max}}$, surpassed only by the Nd-Fe-B magnets. A complementary Curie temperature, T_C, of Sm-Co magnets (above room temperature for all Sm-Co phases) makes them very suitable for high temperature applications. In this work, Sm-Co films were investigated on different substrates. The knowledge of substrate symmetry was exploited, to manoeuvre the growth and orientation of the easy axis (c-axis in Sm-Co) towards a uniaxial growth. Textured films with a remanence as high as 91% of the saturation magnetisation could be achieved on MgO(110) single crystal substrates. A complete overview of the properties, phases and the work done on Sm-Co may be found in chapter 3.

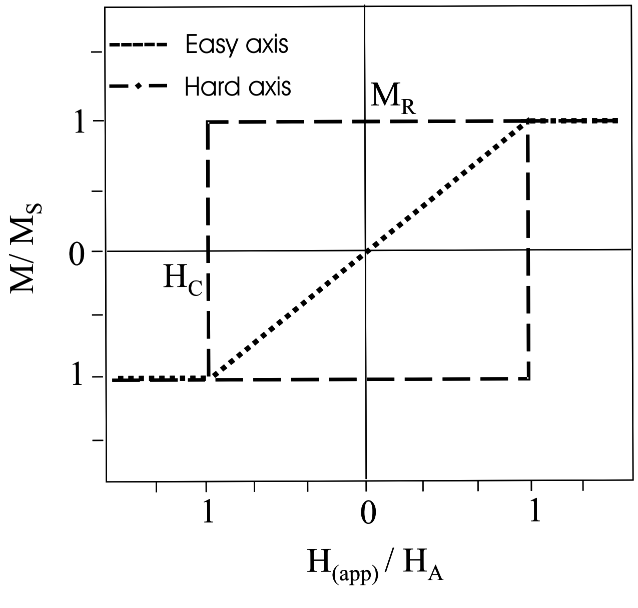

Fig. 1.2: *Hysteresis in an ideal ferromagnet as a M-H loop along the easy magnetisation axis (large* H_C *and high* M_R*) and hard magnetisation axis.*

An equally important requirement for high performance hard magnets is to have a high coercivity, which may be modified by tuning the microstructure (depending on the switching mechanism). An ideal microstructure resulting in high coercivities would require small grain sizes and sufficient pinning sites (for the particular case of Sm-Co films where pinning will be shown to be the magnetisation reversal mechanism) to cause as hard a switching as possible. Pinning defects block domain walls from expanding freely into the hard phase after an easy nucleation and, hence, lead to coercivities that are typically higher than the nucleation fields. And therefore, the higher the density of these defects, the more effective would be pinning in the system, to a first approximation. A schematic microstructure is presented in Fig. 1.3 showing the mechanism of nucleation and pinning in hard magnets. Regions A, B and C present areas where easy nucleation of a reverse domain occurs and the magnetisation is reversed. However, inhomogeneities present in the system shown as pinning centres close to region C, hinder free expansion of this reversed domain, resulting in a delayed overall reversal of the entire sample magnetisation and therefore result in higher coercivities. The magnetisation reversal in the sample in this case is pinning controlled and can be visualised with the help of schematic 1.3b. The domain wall tries to smoothly sweep through the entire sample dimensions causing the already reversed domain to increase in size and the entire sample magnetisation to reverse. But as soon as it encounters a pinning center or a defect in the material where the regular crystal structure is disrupted, the energy barrier for the domain wall to pass through is higher and the domain wall is trapped or pinned until sufficient energy is available to overcome this increased barrier presented by the defect site. Hence, the magnetisation reversal is delayed and occurs at higher externally applied fields. The realisation of this microstructure which contains sufficient effective pinning sites depends on processing kinetics and nature of intrusions/defects introduced.

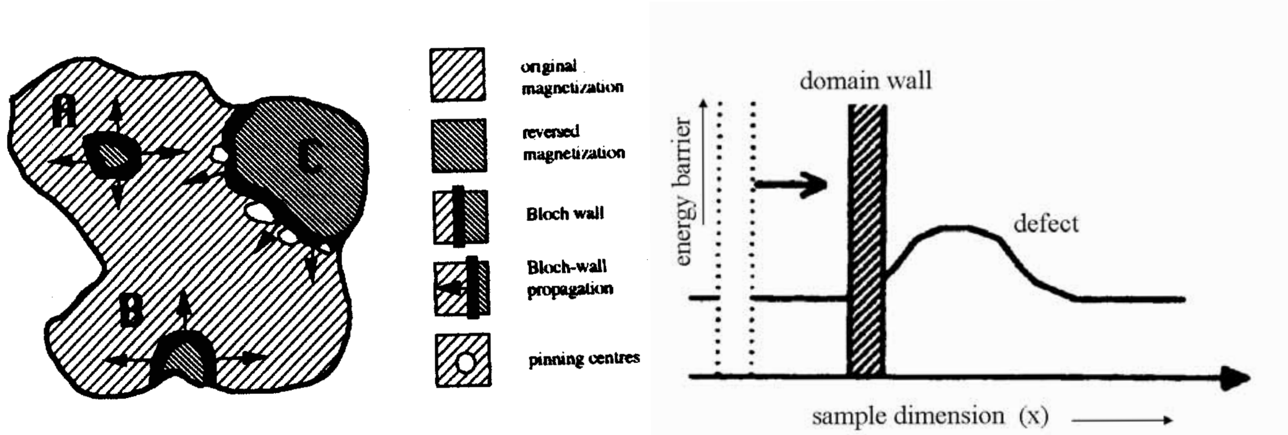

Fig. 1.3: *(a) Hard grain with regions A, B and C showing schematically the beginning of a nucleation process and pinning of a domain wall at pinning sites. (b) Schematic of a domain wall pinned at a defect site due to increased energy barrier at the defect site [Sko99].*

However, even in the best case of most effective pinning, the achievable coercivities are restricted to a third of the total anisotropy field of the magnet (the theoretical externally applied magnetic field at which the magnetisation reversal of the sample occurs) [Kro87]. This limit for a system like $SmCo_5$ (with anisotropy fields = 30 T) would still predict exorbitantly high coercivity values of more than 10 T. Surprisingly $H_C \sim 10$ T has never been observed for $SmCo_5$ and even the highest reported values are well over a factor 3 smaller than these predicted values [Pra99], [Zho00], [Liu02]. This suggests that there still exists a huge room for enhancing the “High" and “Giant" coercivities to even gigantic numbers.

The aim of this work is the preparation of epitaxial hard-magnetic Sm-Co thin film magnets with optimum growth conditions to achieve the best combination of coercivity, remanence and energy products and making a sincere attempt towards correlating the observed global macroscopic properties with the basic magnetisation processes at the microscopic level. Chapter 2 describes the origin of magnetism in these *R*-*T* compounds, followed by a brief discussion of their intrinsic properties (anisotropy field and constants), hysteresis loop, the origin of coercivity and the models available for understanding magnetisation reversal mechanisms. It continues with the basic demagnetisation process for exploring the possibility of intergranular exchange coupling and finally an introduction to one special phase of the *R*-*T* system – the Sm-Co system. Hence, this chapter essentially builds up the necessary infrastructure for subsequent discussion of results in chapter 5 and 6. Chapter 2 is concluded with an overview of the reports available on analysing and interpreting hysteresis loops to get information on magnetisation reversal and inter-grain exchange coupling.

Since a very balanced part of the work focusses on obtaining epitaxial thin films, chapter 3 engages itself with processes involved during thin film deposition, starting with fundamentals of nucleation to factors deciding the growth of continuous films. A short recap into physics of epitaxial films follows thereafter touching only relevant aspects which arise later in chapter 5. This chapter is concluded with a short review on the current status of Sm-Co thin film development.

The experimental techniques involved in the course of this work are fairly described in chapter 4. Chapter 5 contains the main results and discussions pertaining to epitaxial growth of Sm-Co thin films on single-crystal substrates of different orientations using pulsed laser deposition. Chapter 6 is restricted to magnetic measurements that subdivide into analysing the mechanism of magnetisation reversal in these thin-film magnets and evaluating the presence of intergranular exchange coupling through measurement of recoil magnetisation loops and constructing δJ plots. A concise conclusion chapter summarises the most important scientific work of this thesis.

2 Rare-Earth (R) Transition Metal (T) Magnets

The following chapter focusses on the briefest introduction to some of the basic concepts of *R-T* magnetism which are relevant for a successful discussion of results of this work. Through each of these sections, references have been made from [Cul72] for basic understanding of magnetism and [Coe96], [Sko99], [Tre05] for more specialised themes of *R-T* magnetism.

2.1 3d-4f Magnetism in R-T Intermetallics

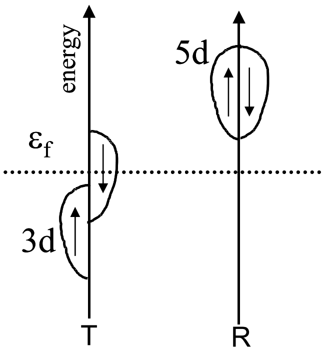

Fig. 2.1: *3d and 5d bands of the transition element and rare earth [Tre05].*

Magnetic coupling in *R-T* compounds is studied by many groups worldwide [Cam72], [Cad87b], [Ric98], [Rad02] due to the interesting phenomenon. The magnetism in these complex intermetallics arises from the coupling between partially filled 3d shells of the transition metal and the 4f of the rare-earth system. Several approaches towards understanding this magnetism have been proposed, but the one from Campbell in 1972 [Cam72], regarding the intervention of 5d electrons of the rare-earth elements, has been most widely accepted.

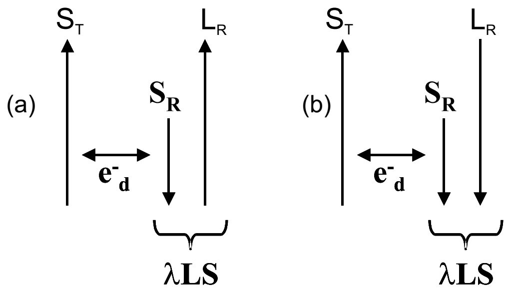

Fig. 2.2: *Total angular momenta of the (a) light and (b) heavy rare earth (R) and the transition metal (T) elements showing that the coupling between transition element and the light rare earth elements is ferromagnetic (case (a)) and anti-ferromagnetic in the case of heavy rare earth and transition element (case (b)) [Tre05].*

The overall coupling is then visualised as a superposition of coupling between the 4f and 5d orbital of the rare earth (intra-atomic coupling) and a second contribution coming from the coupling between the 5d orbital of the rare earth and the 3d orbital of the transition metal (inter-atomic coupling). The 4f-5d coupling (intra-atomic coupling) is always ferromagnetic. The 3d-5d coupling (inter-atomic coupling) occurs through hybridisation of these orbitals. This overlap between the 5d↓ orbital states with those of the 3d↓ is much greater than the corresponding overlap between 5d↑ and the 3d↑ orbitals, since the amount of hybridisation is proportional to the distance between the orbitals (Fig. 2.1). This causes the available d↓ states to be more in number than the available d↑ states resulting in an antiferromagnetic coupling between the 3d and 5d states. The antiferromagnetic 3d-5d coupling causes a strong antiparallel exchange coupling between the 3d spins and 4f spins. Hence, the magnetisations of the light rare earth ($J = L - S$, for light rare earths, as per the Hund's rule) and the transition metal are parallel, and the magnetisation of the heavy rare earth ($J = L + S$) is antiparallel to the transition metal magnetisation leading to an anti-ferromagnetic R-T coupling (Fig. 2.2). The strong ferromagnetic coupling in the light rare earth R-T compounds makes them very attractive permanent magnets because the rare earth's moments can remain ordered to high temperatures (far above room temperature benefitting from the high T_C of transition metals) and the transition metal atoms, which have very low magnetic anisotropy, gain from the high intrinsic magnetic anisotropy of the rare-earths.

2.2 Magnetic Anisotropy

Anisotropy of a material means that the measured properties are different along different crystallographic directions. It is, hence, one key property which decides the shape of its magnetic hysteresis. Anisotropy in hard magnetic materials is essentially of two kinds:

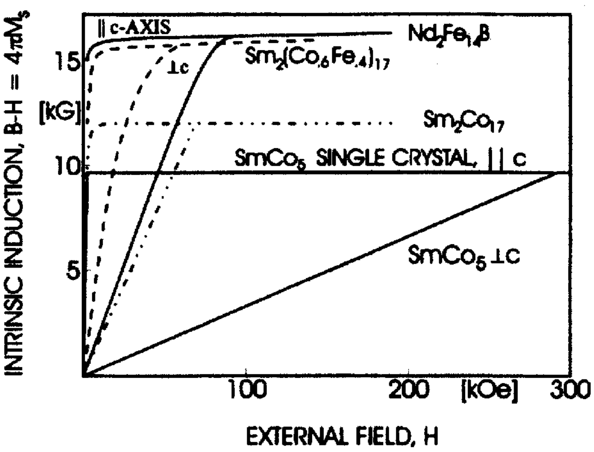

Fig. 2.3: *Intrinsic anisotropy in SmCo$_5$ [Kir96].*

(a) Crystal Anisotropy

Also referred to as magneto-crystalline anisotropy, crystal anisotropy is the cause of intrinsic anisotropy in ferromagnetic materials. It may be viewed as a force that binds the magnetisation to a certain direction (or form of directions) in the crystal. For SmCo$_5$ [Kir96], which has a hexagonal crystal symmetry, the magnetisation increases rapidly with the applied field along the c-axis and attains saturation very fast (Fig. 2.3). This axis, therefore, is called the easy axis since the magnetisation is easy to saturate. But when the field is applied along any other direction in the a-b basal plane, the magnetisation increases at a constant rate (or in other words, the magnetic susceptibility $\chi = \partial M / \partial H$ is low) until it saturates at the same value as for the easy axis. Since it is more difficult to saturate the magnetisation along this axis, it is called the hard axis direction. Both, the easy and the hard axis for SmCo$_5$ are depicted in Fig. 2.3.

The increase in magnetisation occurs through domain wall motion or rotation, and the applied field must do work to turn the magnetisation vector away from the easy direction by a small angle θ. This work gets stored as the crystal anisotropy energy E_{K} and for the specific case of hexagonal crystals with uniaxial anisotropy, it is given as [God65]:

$$E_{\mathrm{K}} = \mathrm{K}_0 + \mathrm{K}_1 \sin^2\theta + \mathrm{K}_2 \sin^4\theta + \mathrm{O}(\theta^6) \tag{2.1}$$

where θ is the angle between the easy axis and the applied field. Hence, E_{K} varies as orders of $\sin^2\theta$ and K_0, K_1, K_2 are the zeroth, first, second order anisotropy constants which measure the weight of the successive $\sin^2\theta$ terms in the anisotropy energy equation. $\mathrm{O}(\sin^6\theta)$ represents the higher order terms in $\sin\theta$. Generally, K_0 is neglected because it is direction independent and K_1, K_2 and other higher order constants are considered if they have significant values.

For the case of Sm-Co, K_2 is much smaller than K_1 and hence K_2 is neglected too. The anisotropy constants are strongly temperature dependent. The measured and calculated temperature dependence of K_1 for SmCo_5 [Szp79] [San75] is shown in Fig. 2.4. Since K_2 is negligibly small, only the calculated temperature dependence of K_2 is presented. Equation 2.1 presents a domain structure where in the demagnetised state the domains point either up or down.

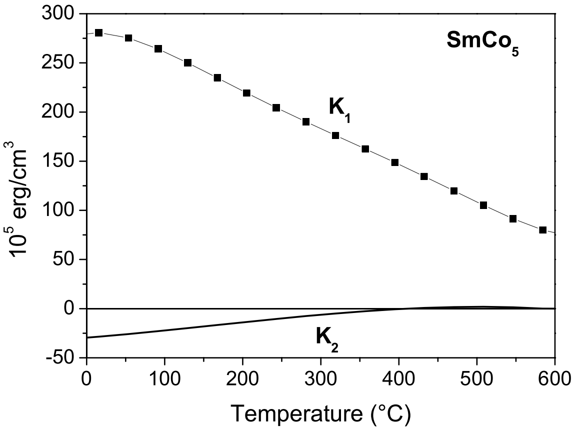

Fig. 2.4: *Calculated and measured temperature dependence of* K_1 *and* K_2 *of SmCo*$_5$ *[Szp79].*

The anisotropy energy can also be expressed in terms of another concept, namely that of an anisotropy field H_{K}, which is the field that reproduces the energy necessary for small deviations from the easy axis. Hence, if a small deviation $\delta\theta$ of the magnetisation M_{S} away from the easy axis changes $E_{\mathrm{K}}(\theta)$ correspondingly to $\delta E_{\mathrm{K}}(\theta)$, then a restoring torque $L(\theta)$ acts on M_{S} in the opposite direction, which tries to decrease θ.

$$-L(\theta)\,\delta\theta = \delta E_{\mathrm{K}}(\theta) \tag{2.2}$$

$$L(\theta) = -\frac{\partial E_{\mathrm{K}}}{\partial\theta} \tag{2.3}$$

Equation 2.1 leads to

$$L(\theta) = -2\mathrm{K}_1\theta \tag{2.4}$$

for small angular deviations θ.

Alternatively, the torque exerted by the anisotropy field H_{K} on M_{S} is the work done by the anisotropy field in restoring the magnetisation again to its easy direction and, hence, is given by the moment of the anisotropy field. Therefore,

$$L(\theta) = -\mu_0 H_K M_S \ \sin\theta \tag{2.5}$$

which for small angular deviations from the easy axis reduces to $-\mu_0 H_K M_S \theta$. And, hence,

$$\begin{aligned} \mu_0 H_K M_S \theta &= 2\mathrm{K}_1 \theta & (2.6) \\ H_K &= \frac{2\ \mathrm{K}_1}{\mu_0 M_S} & (2.7) \end{aligned}$$

The anisotropy field at room temperature of the thin-film magnets under investigation in this work is 28 T, obtained by extrapolating the easy-axis curve and the hard-axis magnetisation curve to intersection. This compares very well with reports from Kirchmayr, Scholz and others [Kir96], [Szp79], [Sch03]. Whereas the anisotropy field takes account of restoration of small angle deviations of the magnetisation from the easy axis, the saturation field H_S is responsible for aligning all the spins along the applied field direction when the field points along a non-easy axis (or more appropriately, the hard axis). Thus, H_S is expressed as:

$$H_S = \frac{2\mathrm{K}_1 + 4\mathrm{K}_2}{\mu_0\ M_S} \tag{2.8}$$

and is theoretically higher than H_K.

(b) Shape Anisotropy

A second and equally important contribution to overall anisotropy in materials comes from the shape or geometry of the sample. Upon magnetising a sample in a strong externally applied field, positive and negative surface charges develop, forming magnetic dipoles in the sample. The direction of magnetic field generated by this dipole is opposite to the magnetisation of the sample. This field which intends to "demagnetise" the sample is called the demagnetising field and is given by

$$H_d = \mathrm{N_d} M_S \tag{2.9}$$

where the coefficient $\mathrm{N_d}$ is the demagnetising factor. It is the second important field that determines the overall anisotropy in ferromagnets besides the intrinsic crystal anisotropy.

The demagnetising field is strongly influenced by the shape/geometry of the sample. For a polycrystalline sample, which has its grains oriented in all possible directions, there exists no overall crystal anisotropy. If it is additionally spherical, the magnetic moments average out and cancel one another. However, if the crystal is non-spherical, it is easier to magnetise it along the long axis as along the short axis due to a smaller demagnetising field along the long axis compared to the short axis. The energy that is associated with the demagnetising field of the sample (prolate ellipsoid) is

$$E_{SF} = \frac{1}{2}\mu_0 M_S^2 N_{\parallel} + \frac{1}{2}(N_{\perp} - N_{\parallel})\ \mu_0 M_S^2 \sin^2\theta \tag{2.10}$$